Songklanakarin J. Sci. Technol.
36 (3), 333-344, May - Jun. 2014

SJST SONGKLANAKARIN JOURNAL OF SCIENCE AND TECHNOLOGY
http://www.sjst.psu.ac.th

Original Article

Joint analysis of shear wave velocity from SH-wave refraction and MASW techniques for SPT-N estimation

Sawasdee Yordkayhun[1,2]*, Chedtaporn Sujitapan[1], and Tanit Chalermyanont[3]

[1] *Department of Physics, Faculty of Science,*

[2] *Geophysics Research Center,*

[3] *Department of Civil Engineering, Faculty of Engineering,*
Prince of Songkla University, Hat Yai, Songkhla, 90110 Thailand.

Received 20 June 2013; Accepted 16 December 2013

Abstract

Horizontally polarized shear wave (SH) refraction and multichannel analysis of surface wave (MASW) methods have been carried out in Hatyai City, southern Thailand, a pilot study for site classification, part of the National Earthquake Hazards Reduction Program (NEHRP). The objectives of this study are the comparison of the efficiencies of different shear wave velocity (Vs) determination techniques and the use of Vs measurements of the prediction of standard penetration resistance (SPT-N). Good correlation between all Vs profiles and SPT-N values and local lithology are observed. However, there are systematic differences between SH-refraction based-Vs and MASW based-Vs, which might be explained by possible converted waves, limitations of the assumptions used, poor quality of the acquired data, and limitations of the inversion procedures of the methods applied. From the integrated use of Vs from both methods an empirical formula to describe the correlation between Vs and SPT-N values has been proposed and can be used to estimate geotechnical parameters in areas where no borehole or geophysical investigation exist.

Keywords: SH-wave refraction, MASW, SPT-N, shear wave velocity, seismics

1. Introduction

From geotechnical engineering point of view, standard penetration resistance (SPT-N) obtained from standard penetration test is a fundamental indicator of soil stiffness and it is recognized in evaluating the ground characteristics for building sites. However, soil classification based on SPT-N value is somewhat qualitative evaluation (Suto, 2011). In addition to the borehole requirement, it is often cost effective and unsuitable to be implemented routinely in urban and large survey area. An alternative method is coming with the use of shear wave velocities (Vs), a quantitative parameter describing the dynamic properties of soils.

Many researchers have shown that Vs can be used in a broad range of applications, including foundation stiffness assessment, earthquake site response, liquefaction potential, site classification for national earthquake hazards reduction programs (NEHRPs), soil compaction, and detection of cavities, tunnels and sinkholes (Seed *et al.*, 1983; Kayabali, 1996; Andrus and Stokoe, 2000; Leparoux *et al.*, 2000; Youd and Idriss, 2001; BSC, 2003; Ergina *et al.*, 2004; Kanli *et al.*, 2006; Anbazhagan and Sitharam, 2008; Karastathis *et al.*, 2010; Sloan *et al.*, 2009; Patel, 2012; Thitimakorn and Channoo, 2012).

Practically, Vs can be determined either in invasive (e.g., downhole or crosshole and suspension PS logging) or

* Corresponding author.
Email address: sawasdee.y@psu.ac.th

non-invasive methods (e.g., surface seismic methods and empirical relation with N-value from Standard Penetration Test, SPT). Disadvantages of the invasive methods are that the measurements are quite expensive and difficult to conduct in urban areas. For seismic methods, SH-wave refraction is considered to be standard technique for Vs determination. However, the velocity inversions, hidden layers problems and interfering of P-wave and S-wave arrivals can lead to the pitfalls in data interpretation. Recently, a new technique for Vs determination, namely multichannel analysis of surface wave (MASW) has been developed (Park *et al.*, 1998). Due to the inherent strong signals of surface wave in shot records and providing a fast and convenient way to evaluate soil stiffness even in urban environment, MASW has been increasingly used. Generally, both SPT-N data and geophysical data do not often exist in a particular area. Statistical analysis of correlation between these parameters is an alternate method (Akin *et al.*, 2011) to estimate SPT-N values or Vs with convenience, less cost, and without additional investigations and data aquisition. Several empirical relationships exist for different lithologies and they appear to be site dependent (e.g., Hasançebi and Ulusay, 2007; Tsiambaos and Sabatanakis, 2011).

As a part of NEHRP soil classification study for Hat Yai city, southern Thailand, Vs data of geological units exposed in this area are essential parts for site response analyses. The average shear wave velocity at the top 30 m of subsurface (Vs(30)) is important in soil classification and characterization according to NEHRP and International Building code (IBC). This parameter can be calculated as follows (Dobry *et al.*, 2000),

$$Vs(30) = \frac{30}{\sum_{i=1}^{n} (h_i / Vs_i)} \qquad (1)$$

where h_i and Vs_i denote the thickness and Vs of the ith layer in the upper 30 m of the total n layers, respectively.

In a preliminary test of the project, shear wave velocities derived from two methods including SH-wave refraction and MASW were tested at three test sites where geotechnical parameters from boreholes have been previously investigated. This test allowed us to compare the performance of the methods for Vs determination. In order to benefit and utilize the geophysical data, beside this comparison, attempt is made to develop the empirical relationship between Vs and SPT-N corresponding to a local scale of the areas based on joint analysis of Vs data from the two methods.

2. Geology

Located in Songkhla Province, southern Thailand, Hat Yai City is known as a principal administrative, commercial, educational and cultural city. The city has been recorded as low seismicity region (Sutiwanich *et al.*, 2012). The average elevation of this area is about 0-20 m above mean sea level. Hatyai City is part of the Hat Yai Basin, which is formed by the horst-graben structures. Morphological evidences come from the surrounding north-south trending mountain ranges (Sawata *et al.*, 1983). The eastern and western boundaries can be characterized by granite intrusions and metamorphic rocks that act as the basin basement. The basin geometry estimated from geophysical studies is approximately 60 km long, 20 km wide and 1 km deep filled with sediments of Carboniferous to Triassic age (Lohawijarn, 2005). These units are covered by Quaternary deposits consisting of semi-consolidated clay, silt, sand, and gravel. Unconsolidated Quaternary sediments found in this area are useful in site investigation, foundation, groundwater and environmental studies.

The Quaternary alluvial unit (Qa) and colluvium unit (Qc) broadly cover the study area (Figure 1). The test sites are located in the colluvium unit, consisting of unconsolidated sediment of sand, gravel, clay and silt that are partly weathered from host rock and mostly found near the hill and outcrop boundaries (Saardsud and Srisangjun, 2002).

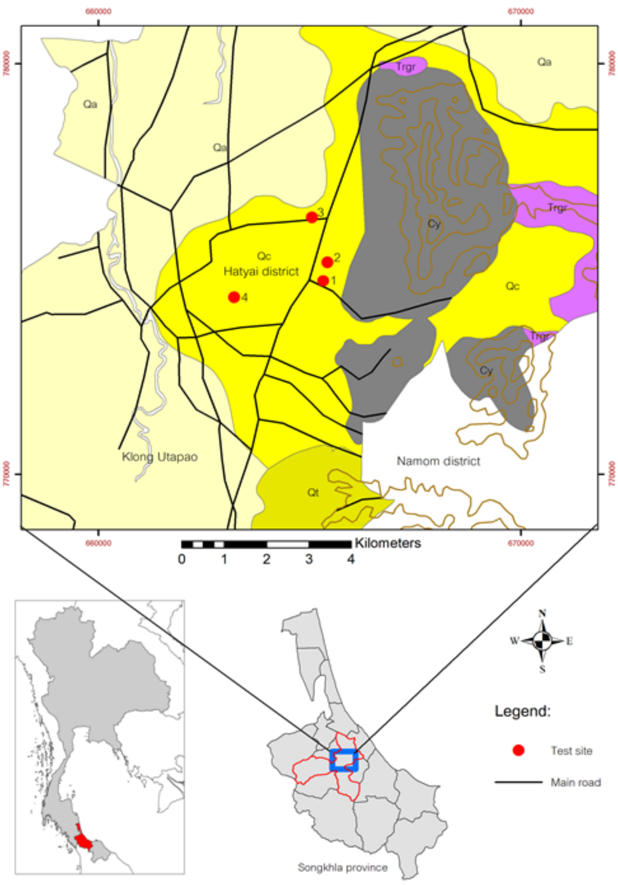

Figure 1. Geologic map of study area showing the test site locations (red dot). Descriptions for the geological units are as following: Qa = Alluvial deposits: Quaternary, Qc = Colluvial deposits: Quaternary, Qt = Terrace deposits: Quaternary, Cy = Shale, chert and conglomerate: Carboniferous, and Trgr = Granite: Triassic.

3. Methods

3.1 SH-wave refraction method

Seismic refraction method is a common method applied for near surface investigations. The principle of the method uses refracted wave across the boundary between layers of different physical properties governing the Snell's law and Huygen's principle. By recording elastic waves using a series of geophones placed on the ground (Figure 2a), seismic traveltime versus distances can be recorded and used as input for data interpretation. A number of techniques have been available for data interpretation, including intercept time method (Hagedoorn, 1959), reciprocal or delay time method (Hawkins, 1961; Palmer, 1980), ray tracing method (Leung, 1995), and inversion and tomography method (Zhang and Toksöz, 1998; Yordkayhun *et al.*, 2009; Yordkayhun, 2011).

In this study, SH-refraction data were recorded using a 24-channel Geometrics Smartseis seismograph. Twelve 14-Hz horizontal component geophones were deployed at 5 m intervals and oriented in orthogonal to the direction of wave propagation during acquisition. The S-wave was generated by hitting the ends of a wooden timber (shear wave impact plate) laid perpendicular to the geophone spread. Shot points were located at five positions, including near and far offset on both ends and at the center of the geophone line. Vertical stacks (or hammer blows) were done at each shot point to enhance the signal to noise ratio. Table 1 summarizes acquisition parameters used for this study.

In this work, Vs model was generated based on tomography methods (Yordkayhun, 2011). The first arrivals to each geophone were picked and used as input to reconstruct the velocity model based on a non-linear least squares inversion. Both automatic and manual picking were performed to avoid picking error at the far offset traces. The inversion procedures started from estimation of an initial model. We used simple two-layer velocity models produced by the time-term method as an initial model to constrain the reliability of the tomographic inversion. Next, predicted traveltimes (forward model) were calculated. The calculated traveltimes were then compared to the observed traveltime. The residuals between them were minimized by updating the model through the iterative inversion process until the acceptable model was obtained. In this study, each inversion was run with 10 iterations. By testing on the initial model, RMS errors between the picked and calculated traveltimes are in the range of 2-5 ms and final model converges within five iterations.

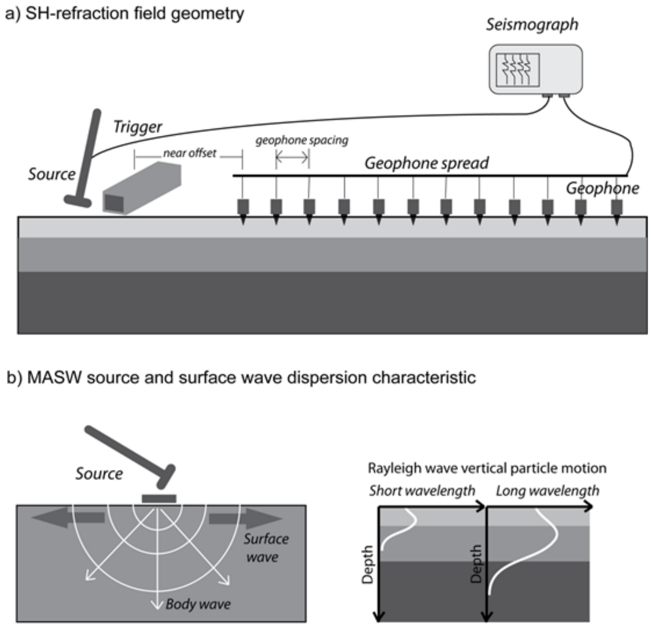

Figure 2. (a) SH-refraction field geometry. Note that SH-wave energy source and horizontal geophone are used. (b) MASW energy source is similar to the conventional P-wave energy source (left). The surface wave generated from this source has dispersion characteristic (right).

3.2 MASW method

MASW method utilized phase velocity of surface wave (Rayleigh wave or ground roll) that are typically considered as noise for seismic surveys, to estimate Vs profiles (Park *et al.*, 1998). Rayleigh wave phase velocity is a

Table 1. Acquisition parameters and equipment.

Parameter	SH-refraction	MASW
Energy sources	10 kg sledgehammer	10 kg sledgehammer
Shot spacing	30 m	30 m
Natural frequency of geophone	14 Hz (horizontal)	14 Hz (vertical)
Geophone spacing	5 m	2.5 m
Offset Min/MaxField geometry	2.5/60 mFixed spread	2.5/60 mFixed spread
Recording system	Geometric SmartSeis	Geometric SmartSeis
No. of channels	12 channels	24 channels
Record length	1,000 ms	1,000 ms
Sampling interval	0.5 ms	0.5 ms

function of frequency and subsurface properties including Vp, Vs, density, and layer thickness. In a homogeneous medium, a Rayleigh wave has phase velocity ranges from 0.87 to 0.96 of Vs (Richart *et al.*, 1970) over a range of Poisson's ratio, whereas it has dispersion characteristics in a vertically heterogeneous medium (Figure 2b). MASW data are recorded as the same manner as the conventional seismic reflection/refraction acquisition (Figure 2a), except the low natural frequency geophone (~4.5 Hz) is typically used (Xia *et al.*, 1999).

In this study, MASW data were acquired at the same location and similarly oriented with SH-refraction recording. Data were recorded with twenty-four 14-Hz vertical component geophones with the geophone spacing and the near offset of 2 m and 2.5-10 m, respectively. The source was a sledgehammer vertically hitting a metal plate (Figure 2b). Shot points were located at both ends of the line. Acquisition parameters used for this study is outlined in Table 1. The MASW data processing relies on the principles of the dispersion analysis and inverse theory described by Park *et al.* (1998) and Xia *et al.* (1999). First, dispersion energy was generated using wavefield transformation of a shot gather from time-space (t-x) domain to phase velocity-frequency (f-v) domain. In this method, the Fourier transformation was applied to the time axis of the shot gather and slant stacking with different values of slowness was applied to obtain the phase velocity for a particular frequency and the maximum stacked amplitude is a result of the determined slowness. Then a dispersion curve was picked at the peaks of dispersion energy over different frequency values and quality control was done by considering the fundamental mode surface waves of the signal and their signal to noise ratio. After that, an iterative weighted least-squares inverse of dispersion curve was performed by setting up a suitable initial model and adjusting the model parameter values (the Vs) with the objective of minimizing the error between the calculated and picked dispersion curve. For inversion algorithm, we used gradient iterative solutions to the weighted equation by the Levenberg–Marquardt (L-M) and the singular-value decomposition (SVD) techniques (Xia *et al.*, 1999). Xia *et al.* (1999) mentioned that surface wave data are not sensitive to Vp and density, thus a five-layer model with fixed Poission's ratio and density of 0.40 and 2.0 g/cm^3, respectively were chosen for the inversion. After 10 iterations, a final 1D velocity profile locating at the middle of the geophone spread was obtained.

Apart from MASW analysis, the first arrival times of the same shot gathers can be used to establish P-wave velocity (Vp) model since forward and reverse shots of MASW records were performed as the same manner as the SH-refraction geometry. Note that the Vp model was generated based on tomographic inversion using the initial model derived from the traveltime curves.

3.3 Relationship between Vs and SPT-N values

Over the few decades, SPT-N value estimation for different soil types has been derived from Vs by means of an empirical relation (Ohta *et al.*, 1978; Imai and Tonouchi, 1982; Kokusho and Yoshida, 1997; Hasançebi and Ulusay, 2007; Dikmen, 2009; Brandenberg *et al.*, 2010; Maheswari *et al.*, 2010; Akin *et al.*, 2011; Suto, 2011; Tsiambaos and Sabatanakis, 2011; Marto *et al.*, 2013). These relationships are generally expressed in the power–law forms of:

$$V_s = aN^k \tag{2}$$

In the log scale it can be written as

$$\ln V_s = \ln a + k \ln N \tag{3}$$

where a and k are constants that can be practically determined by performing linear regression to the cross plots of SPT-N values and Vs in the log-log space. The variations of relationships depend on the samples and influence of lithology, soil type, age, and depth (Tsiambaos and Sabatanakis, 2011). However, this study concentrates on the correlations which are only applicable for all soil types and regions. Therefore, the empirical formula developed by integrating 27 published correlations around the world including from Japan, U.S.A., Greece, Taiwan, Turkey, India, Iran, South Korea, and others, were used for comparison with our results and was given for all soil types as (Marto *et al.*, 2013):

$$V_s = 93.67N^{0.389} \tag{4}$$

Note that Equation 4 utilizes the statistical analysis of existing Vs-N value correlations deriving from various techniques, including invasive and non-invasive methods as well as laboratory test. Even though the empirical correlations at local scale for various regions tend to be site dependent, we believe that the established universal correlation can be used as a guideline for any region where the existing correlations are not available.

4. Results and Discussions

4.1 Comparison of the Vs from SH-wave refraction and MASW methods

By comparing raw shot gathers (Figure 3a and 4a), the signal to noise ratio of MASW data is relatively higher than that of SH-refraction data. The dominated high amplitude, low frequency surface wave in the MASW data make dispersion curve able to pick easily, whereas the first arrivals at the far offsets in SH-refraction data are not clear to pick. This implies that the source energy is slightly lower or attenuation of shear wave energy is higher at a long distance. First break pick accuracy has effects on the final results, especially when low frequency data are encountered. We estimated picking uncertainties using dominant frequency of the raw

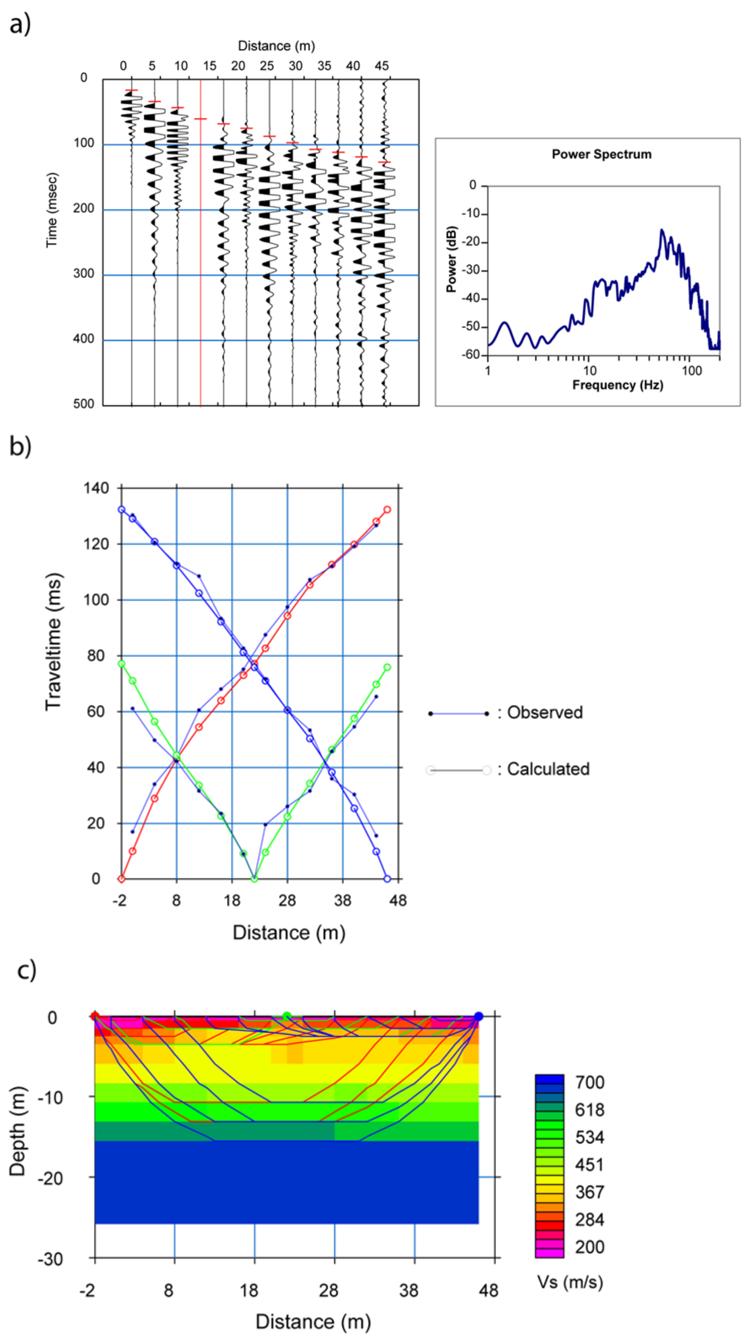

Figure 3. SH-wave velocity model from tomographic analysis. (a) Raw shot gather with first arrivals picked and power spectrum of the signal. (b) Comparison of calculated and observed data. (c) Final tomography model with ray coverage.

data and evaluating the reciprocity of traveltimes (Figure 3b). In Figure 3a, power spectrum of the signal shows dominant frequency in a range of 20–100 Hz, suggesting a picking error on the order of 3–10 ms according to the one quarter dominant period criterion. The effects of source energy limitation are noticeable at far offset shots, when traveltimes could not be picked accurately. Thus, depth of investigation (ray coverage) was limited at some test sites (Figure 3c). For MASW data, however, the penetration depth may be also limited due to the lack of low frequency component of surface wave (no dispersion energy below 5 Hz). Although frequency bandwidth of surface wave are observed in the range of 5–25 Hz in dispersion curve (Figure 4b), examining the power spectrum in the MASW data showed that energy below 5 Hz is greatly attenuated by 30 dB (Figure 4a). This indicates that the natural frequency of the geophones (14 Hz) and the active MASW source have some effect on the data. In fact, if 14 Hz geophones are critically damped, Uyanik

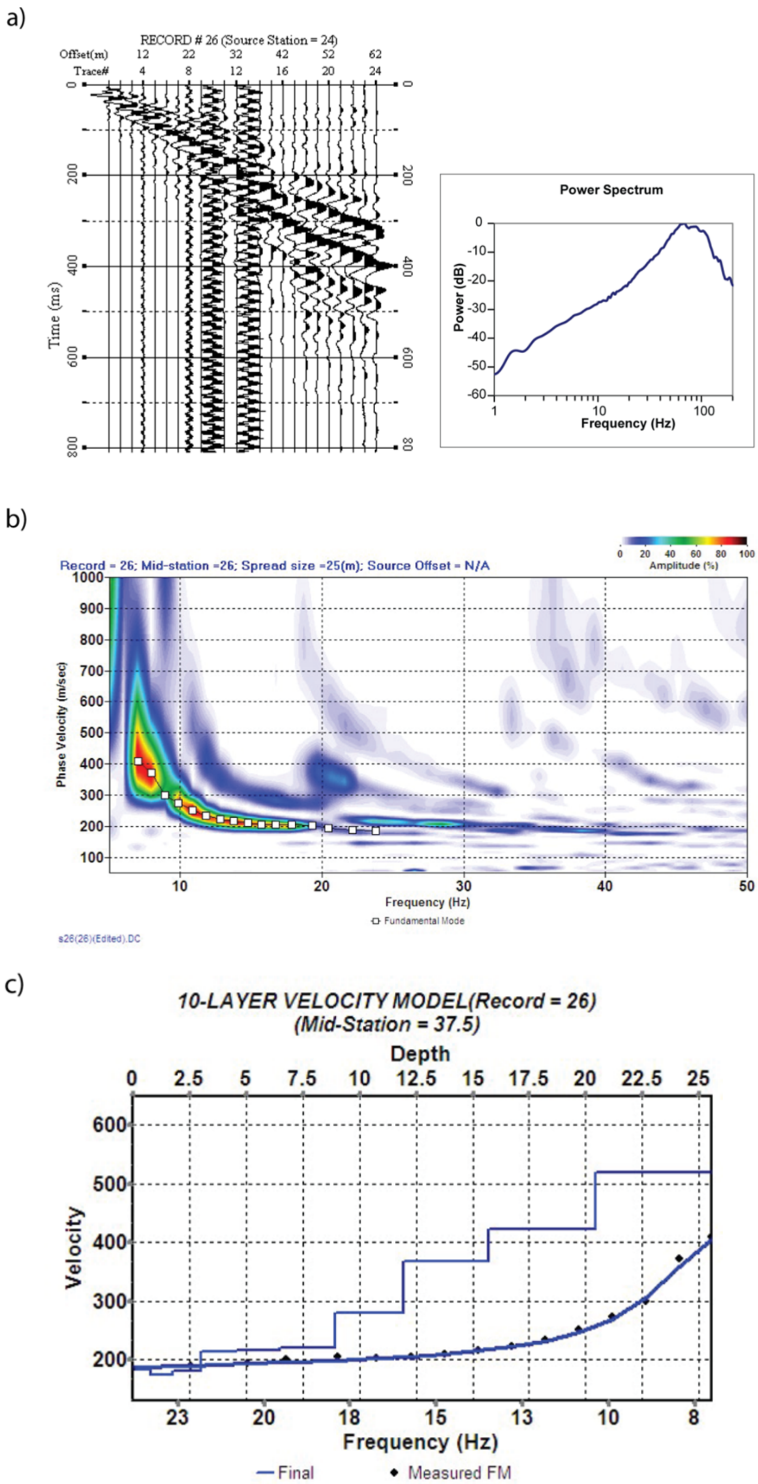

Figure 4. MASW data processing steps. a) Raw shot gather with power spectrum of the signal, b) dispersion characteristics and picking and c) final Vs model.

et al. (2013) pointed out that the signal to noise ratio of data would be valid down to 7 Hz since the relative velocity response of the geophones at 7 Hz would be attenuated by 12 dB. Some apparent errors may be also the results of dispersion curve picking because low frequency random noise can smear the dispersion energy. In Figure 4, assuming 10 Hz is minimum frequency that was picked with high confidence (signal to noise ratio of higher than 0.6) and corresponding phase velocity of Rayleigh wave is 400 m/s, maximum depth of investigation (one-half of the longest wavelength) would be about 20 m. Consequently, combining a passive MASW source with lower natural frequency geophones might be recommended to improve the accuracy at greater depth. Passive surface wave techniques measure low frequency noise field that can originate from many directions, such as ocean wave, traffic, factory activities and wind. Therefore, geophone arrangement in a two-dimensional array (e.g., triangle, circle, semi-circle and “L-shape” arrays) provides a reliable estimation of surface wave phase velocity with a relatively small number of geophones. However, for active source, investigation using linear array and a large energy source is somewhat difficult, particularly in urban environment.

Inverted Vs profiles for the three test sites (Site 1 to 3) along with Vp, SPT-N values and lithology are illustrated in Figure 5. It is noted that the maximum depths of investigation varied from site to site and only the portion of data that respective borehole depth is displayed for comparison. The general trend of linearly increasing velocity with depth of both Vs data sets are approximately the same beyond the borehole depth. Structurally, the Vs profiles are in the good agreement with SPT-N values for all test sites. Low N value and Vs correspond to loose materials which are found at

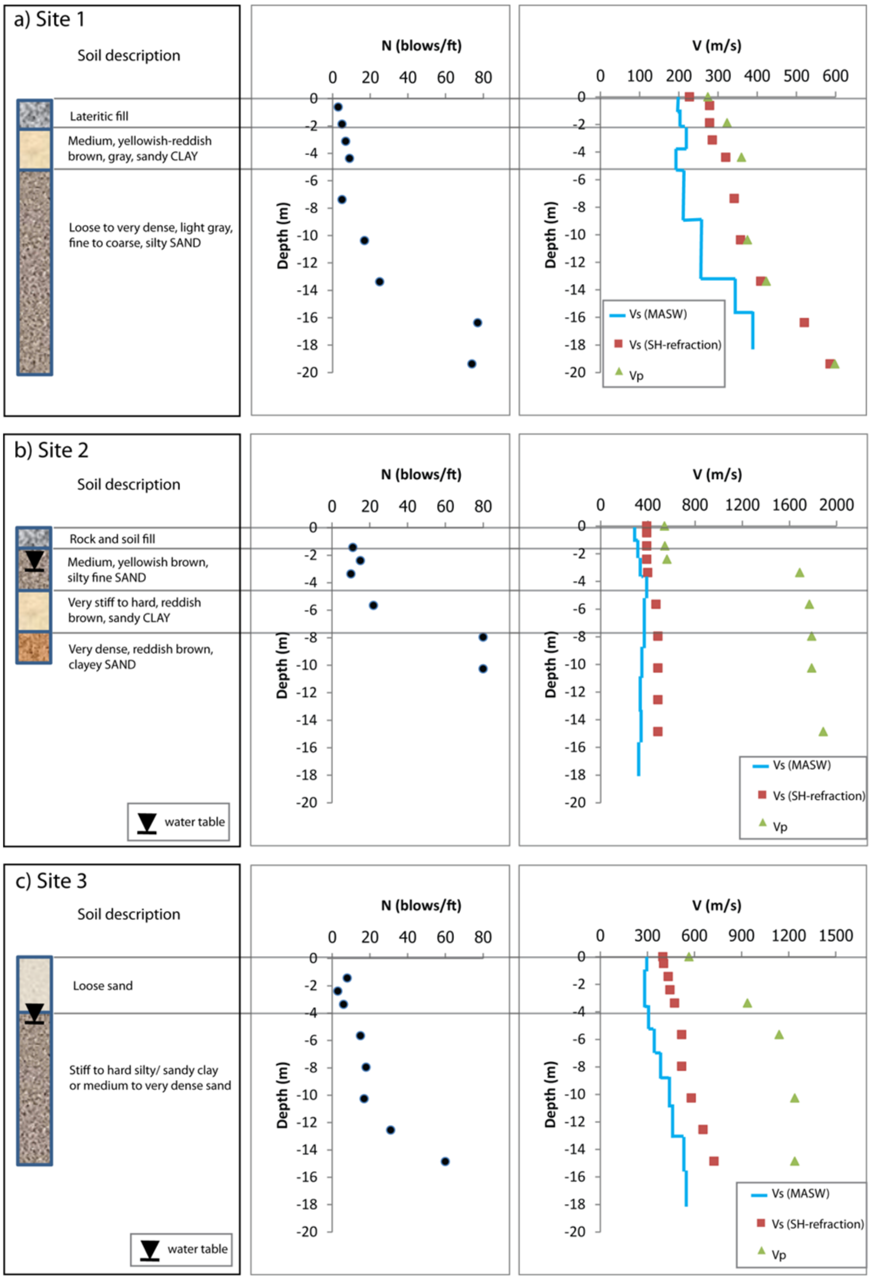

Figure 5. Correlation of Vs and lithology, SPT-N, and Vp for the three test sites.

near surface. Note that the SH-refraction based-Vs (range of about 300-700 m/s) are characterized by relatively higher values (by 28% on average) than MASW based-Vs (range of about 200-500 m/s). These results are consistent with observation by the other studies (e.g., Turesson, 2007). Regarding to this systematic difference, we consider that the Vs from SH-refraction is slightly overestimated due to its assumption and inversion error as mentioned by Schwenk *et al.* (2012). For the assumption error, the layer may be misinterpreted as incorporating a hidden layer, resulting in the layer thickness or velocity may increase. This evidence can be seen in Site 1 and 2 (Figure 5b) where a case for Vs inversion is observed, corresponding to a low-velocity sand beneath a high-velocity clay layer. Also, a low-velocity near-surface layer can cause its depth and velocity to be overestimated as mentioned by Yordkayhun *et al.* (2009). Static corrections for tomographic inversion algorithm may improve accuracy and resolution of the results. For the i nversion error, resolution is often degraded and has artifacts resulting from ray coverage and smoothing imposed to stabilize the inversion. However, Turesson (2007) mentioned that in case of a sharp high-contrast boundary traditional refraction methods are suitable. In this study, abruptly changing soil stiffness may exist as seen by the high N values at the deepest layer. If this is the case, Vs determined by MASW may degrade due to the assumption of constant Poisson's ratio used in the inversion.

It is interesting to note that a part of SH-wave energy is possibly converted into P-wave energy propagating along the interface in case the dipping layers are present (Xia *et al.*, 2002). This can be verified by the Vp and SH-refraction based-Vs that are very close to each other as observed in Site 1 (Figure 5a). Besides tracking the Vp/Vs values, the Poisson's ratio (s) can be determined simply by:

$$\sigma = \frac{V_p^2 - 2V_s^2}{2(V_p^2 - V_s^2)} \quad (5)$$

At Site 2 (Figure 5b), the abrupt change in Vp of slightly higher than 1,500 m/s and the calculated Poisson's ratio of higher than 0.4 indicates water saturated layer below 3 m depth. Generally, Vs are less affected by water table or by pore fluids than Vp since fluids have no resistance to shear (Sheriff and Geldart, 1995). Here, the depth to water table estimated from Vp may differ from the borehole information since they were observed at different times. However, the high Vp/Vs values that characterized depths below 4 m in Site 3 (Figure 5c) would be subjected to layers with high clayey–silt content as mentioned by Sinnanini and Torrese (2004).

To obtain a more quantitative comparison, the Vs(30) is considered because it is representative indicator in the site classification and building codes. The Vs(30) and NEHRP site classification obtained from the MASW and SH-refraction analyses conducted in the test sites are listed in Table 2. According to the Vs(30), all test sites are defined as dense soil and soft rock (site class C) based on SH-refraction data, while two test sites are found to be stiff soils (site class D) based on MASW data. Discrepancies between the two methods indicate the systematic difference of the derived Vs. To assess the reliability of Vs(30), we compare the derived Vs(30) values with the global Vs(30) map provided by the USGS (2013). Although the global Vs(30) map was developed based on correlation between topography and surficial geology which its spatial resolution of about 1 km, it can be used as a guideline value for site assessment in the area. It is clearly seen that the picked global Vs(30) at the test sites (Table 2) tent to have better agreement with Vs(30) from MASW data. However, it is possible that variations in subsurface lithology partially contributed to the overestimation of Vs(30). Since the hard rock is found to be less than 30 m depth at the test sites, Vs of the lowermost layer was assumed for the rest of the depth.

4.2 Empirical relationship between Vs and SPT-N values at the test sites

At the beginning of the Vs-N correlation development from geophysical data, three main groups according to the two methods and the average model were considered. Vs results derived from SH-refraction, MASW and average model are plotted against SPT-N values in the normal and log-log scale in order to develop an empirical relationship (Figure 6). The distributions of Vs with SPT-N value suggest the non-linear relationship between the two parameters. The following power–law expressions were proposed:

Table 2. Comparison of Vs(30) and NEHRP site classification based on Vs derived from geophysical methods and USGS database at the test sites.

Test site: location (UTM, WGS 84, Zone 47)	Vs(30) (m/s)			NEHRP site class		
	SH-refraction	MASW	USGS	SH-refraction	MASW	USGS
Site 1: (665313, 774719)	411	310	310	C	D	D
Site 2: (665416, 775159)	466	337	289	C	D	D
Site 3: (665051, 776255)	596	472	302	C	C	D

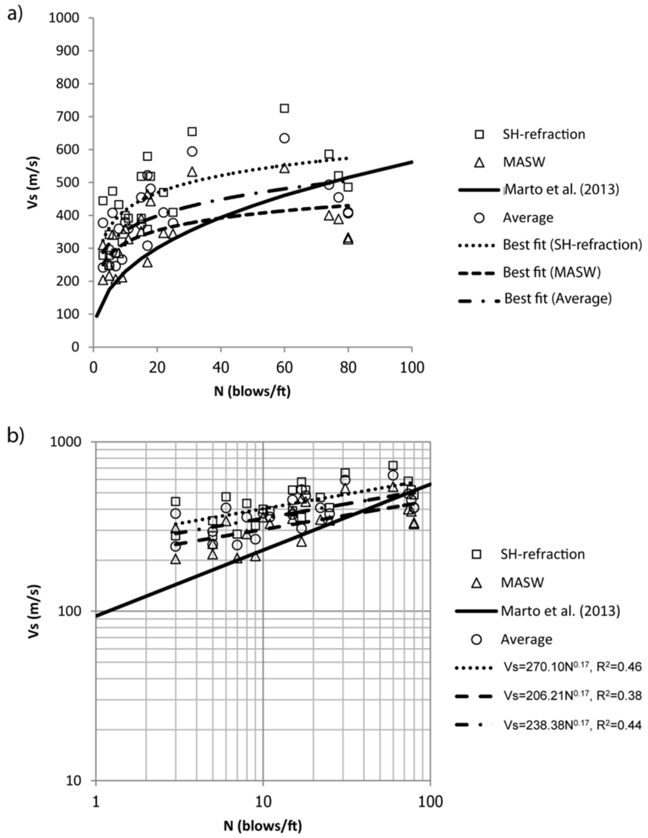

Figure 6. Relationship between Vs and SPT-N values displaying in normal (a) and log-log scale (b).

$$V_s = 270.10N^{0.17}$$, for SH-refraction (R^2=0.46) (6)

$$V_s = 206.21N^{0.17}$$, for MASW (R^2=0.38) (7)

$$V_s = 238.38N^{0.17}$$, for average model (R^2=0.44) (8)

In these relationships, the curvature of the relationship controlling by the exponent values (b) appear to be consistent, while the constant that controls the amplitude (a) are different. This implies that the correlations are mostly affected from the derived Vs values.

As seen in Figure 6, the smallest deviation of Vs for MASW data from the proposed relationship of Marto *et al.* (2013) suggests that the Vs values from MASW are more reliable. It should be noticed that the relationship from the average model has a slightly higher correlation coefficient compared to the ones from MASW. This reveals the influence of statistical analysis in the relation development.

To account for the reliability of Vs from MASW, number of data samples and systematic differences between the two methods, an adapted relationship was considered. Accordingly, a cross plot between the Vs values from the two methods is used to identify their correlation (Figure 7a). A simple linear correlation between the two data sets is proposed as:

(MASW based-Vs) = 0.75 (SH-refraction based-Vs), (R^2=0.89) (9)

By adjusting the Vs from SH-refraction to the Vs from MASW using Equation 9, the Vs-N distribution is presented in Figure 7b. Consequently, the proposed empirical relationship for the test sites can be written as:

$$V_s = 204.39N^{0.17} \tag{10}$$

and its reciprocal is

$$N = \left(\frac{V_s}{204.39}\right)^{5.88} \tag{11}$$

Joint analysis of the Vs from both methods provide remarkable better data fit (R^2=0.42) than the equations based on MASW data alone (R^2=0.38) (Figure 6b). Although data errors may be introduced by this statistical analysis, we observed that the exponent constant value in the adapted relationship is stable. Moreover, the constant that control it's amplitude slightly converge to the proposed equation of Marto *et al.* (2013).

4.3 Verification of the developed empirical relationship

The Vs profile from MASW data of Site 4 is selected to verify the reliability of the developed empirical formula.

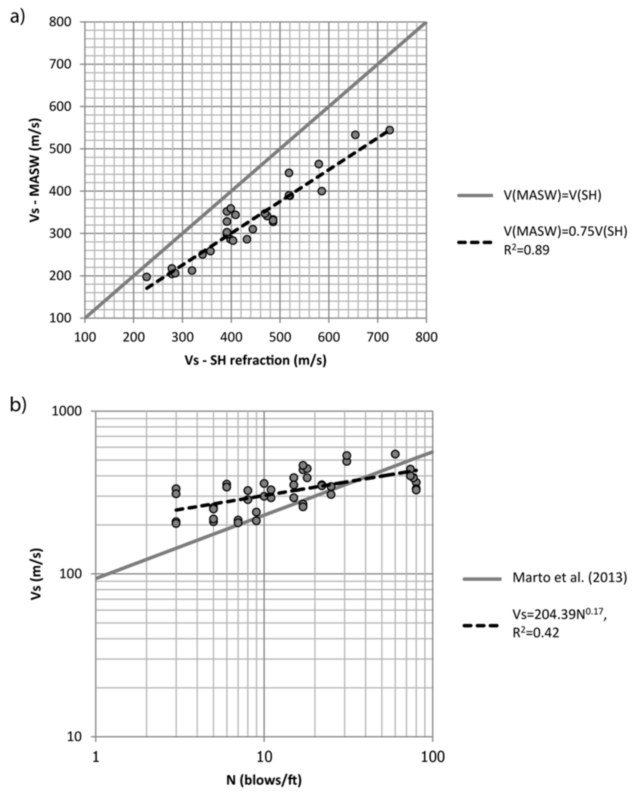

Figure 7. a) Cross plot of the Vs from MASW and the Vs from MASW data. b) Relationship between joint analysis of Vs and SPT-N values.

Figure 8 shows comparison of the measured and the predicted SPT-N values based on Equations 6-10 (present study) and Equation 4 (Marto *et al.*, 2013). The general trends of the predicted SPT-N values appear to be similar and consistent with lithology information. It is seen that the predicted N values based on the developed formula are almost equal to the measured N values beyond 11 m depth (the first layer), whereas the predicted N values according to Marto *et al.* (2013) fit the observed data quite well below 11 m depth (the second layer). This suggests that the effect of soil types and depth may be significant.

In an attempt to consider the depth effect, multiple regression analysis was performed on the adjusted MASW data. Assuming the Vs is influenced by SPT-N value and depth (z), the power-law form can be proposed as:

$$V_s = 209.96 N^{0.105} z^{0.076}, \quad (R^2=0.45) \qquad (12)$$

The comparing results of the newly adapted formula including depth effects (purple line in Figure 8) confirmed that depth has small effect on the N value prediction in this area since the predicted N values became diverge from the measured N values. Thus, it can be concluded that the depth-independent formula (Equation 10 and red line in Figure 8) appear to be reasonable agreement, especially for low N values. This means that soil types and variations play a major role in the Vs-N value correlation as observed elsewhere (e.g., Anbazhagan *et al.*, 2013). Adding more data from different sedimentary units is advisable to improve the accuracy of the developed formula. However, it is insufficient to judge that the present study does not have the potential for application due to the fact that the existing N values have been determined more than 10 years ago at this site. Mismatch of N values at the deeper subsurface might be due to partly land usage and filling.

5. Conclusions

Vs profiles at the test sites have been determined to provide data for site response analyses as part of the NEHRP site classification study in Hat Yai City. SH-wave refraction and MASW methods were tested where the SPT-N values from in–situ measurements were available. This test provides the opportunity to assess the methods efficiency and to develop the empirical relationship between Vs and SPT-N values in the area. The major conclusions are discussed below:

1) Field implementations of the two methods are comparable, except the source energy has some precautions when deeper investigation is needed.

2) Although there are good agreement between the Vs, SPT-N values and lithology at the test sites, it appears to be systematic differences between the two methods as the SH-refraction based-Vs are characterized by higher values than the MASW based-Vs. Discrepancies of Vs from the two methods could be contributed to several reasons, including assumptions used, site-specific differences, data quality, and inversion processes.

3) Pitfalls in Vs determination from SH-refraction data are hidden layers and statics problems, mode conversion of waves, accuracy of picking first arrivals, setting up a reasonable initial model and stability of inversion. Whereas the pitfalls in Vs determination from MASW data are interference of random noise, lacking of the low frequencies surface wave, accuracy of picking dispersion curve, setting up a reasonable initial model, and stability of inversion.

4) Based on comparison of Vs(30) with the global Vs(30) map, lithology information and comparison with the Vp, reliable of Vs at the upper 20 m depth using MASW are promising. However, in case a strong Vs contrast exist at shallow depth, the Vs for the basement from the SH-refraction appear to be better than that of the MASW.

5) Combining the two methods of Vs determination, the empirical correlation between Vs and SPT-N has been expressed as a power equation. This formula can be used to estimate SPT-N values in the area and vicinity where in–situ tests could not be carried out in some restricted areas. Furthermore, geophysical based-Vs is considered to be a non-invasive, cheaper, and faster method compared to borehole investigations.

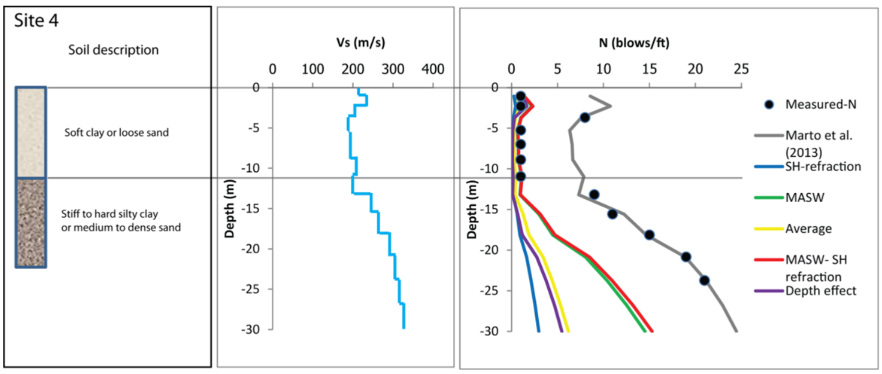

Figure 8. Comparison of the measured SPT-N values and the predicted SPT-N values at Site 4 based on SH-refraction, MASW, average model, joint model (red line), depth effect model (purple line) and Marto et al. (2013).

6) The empirical formula presented here still has significant uncertainties and has been applied as the representative of all soil types within the specific geological unit. To gain a higher confident among geophysicists and geotechnical engineers, the inclusion of more samples, related information from soil types and more reliable of Vs at the greater depth would be recommended for future improvement.

Acknowledgements

This study was supported by Prince of Songkla University (PSU) research grants, contract no. SCI550150S. We would like to thank Department of Physics, Faculty of Science, PSU, for supporting the field equipment. Anonymous reviewers are thanked for their helpful comments and suggestions in improving the manuscript.

References

Akin, M.K., Kramer, S.L. and Topal, T. 2011. Empirical correlations of shear wave velocity (Vs) and penetration resistance (SPT-N) for different soils in an earthquake prone area (Erbaa-Turkey). Engineering Geology. 119, 1–17.

Anbazhagan, P. and Sitharam, T.G. 2008. Mapping of average shear wave velocity for Bangalore region: a case study. Journal of Environmental and Engineering Geophysics. 13 (2), 69–84.

Anbazhagan, P, Kumar, A. and Sitharam, T.G. 2013. Seismic Site Classification and Correlation between Standard Penetration Test N Value and Shear Wave Velocity for Lucknow City in Indo-Gangetic Basin. Pure and Applied Geophysics. 170, 299-318.

Andrus, R.D. and Stokoe, K.H. 2000. Liquefaction resistance of soils from shear-wave velocity. Journal of Geotechnical and Geoenvironmental Engineering. 126, 1015-1025.

Brandenberg, S.J., Bellana, N. and Shantz, T. 2010. Shear wave velocity as function of standard penetration test resistance and vertical effective stress at California bridge sites. Soil Dynamics and Earthquake Engineering. 30, 1026–1035.

Building Seismic Safety Council (BSC). 2003. NEHRP Recommended Provisions for seismic regulations for new buildings and other structures, Part1: Provisions, FEMA 368. Federal Emergency Management Agency. Washington, D.C., U.S.A.

Dikmen, U. 2009. Statistical correlations of shear wave velocity and penetration resistance for soils. Journal of Geophysics and Engineering. 6, 61–72.

Dobry, R., Borcherdt, R.D., Crouse, C.B., Idriss, I.M., Joyner, W.B., Martin, G.R., M.S., P., Rinne, E.E. and Seed, R.B. 2000. New site coefficients and site classification system used in recent building code provisions. Earthquake Spectra. 16(1), 41-68.

Ergina, M., Ozalaybeya, S., Aktara, M. and Yalc, M.N. 2004. Site amplification at AvcVlar, Istanbul, Tectonophysics. 391, 335– 346.

Hagedoorn, J.G. 1959. The Plus-Minus method of interpreting seismic refraction sections. Geophysical Prospecting. 7, 158-182.

Hasancebi, N. and Ulusay, R. 2007. Empirical correlations between shear wave velocity and penetration resistance for ground shaking assessments. Bulletin of Engineering Geology and the Environment. 66, 203–213.

Hawkins, L.V. 1961. The reciprocal method of routine shallow seismic refraction investigations. Geophysics. 26, 806-819.

Imai, T. and Tonouchi, K. 1982. Correlation of N-value with S-wave velocity and shear modulus. Proceedings of the 2nd European Symposium of Penetration Testing, Amsterdam, The Netherlands, May 24-27, 1982, 57–72.

Kanli, A.I., Tildy, P., Pronay, Z., Pinar, A. and Hemann, L. 2006. Vs30 mapping and soil classification for seismic site effect evaluation in Dinar region, SW Turkey. International Journal of Geophysics. 165, 223–235.

Karastathis, V.K., Karmis, P., Novikova, T., Roumelioti, Z., Gerolymatou, E., Papanastassiou, D., Liakopoulos, S., Tsombos, P. and Papadopoulos, G.A. 2010. The contribution of geophysical techniques to site characterisation and liquefaction risk assessment: Case study of Nafplion City, Greece. Journal of Applied Geophysics. 72, 194–211.

Kayabali, K. 1996. Soil liquefaction evaluation using shear wave velocity. Engineering geology. 44, 121-127.

Kokusho, T. and Yoshida, Y. 1997. SPT N-value and S-wave velocity for gravelly soils with different grain size distribution. Soils Found. 37, 107–113.

Leparoux, D., Bitri, A. and Grandjean, G. 2000. Underground cavities detection: a new method based on seismic Rayleigh waves. European Journal of Environmental and Engineering Geophysics. 5, 33–53.

Leung, T.M. 1995. Examination of the optimum XY value by ray tracing. Geophysics. 40, 1151–1156.

Lohawijarn, W. 2005. Potential ground water resources of Hat Yai Basin in Peninsular Thailand by gravity study. Songklanakarin Journal of Science and Technology. 27, 633-647.

Maheswari, R.U., Boominathan, A. and Dodagoudar, G.R. 2010a. Seismic site classification and site period mapping of Chennai City using geophysical and geotechnical data. Journal of Applied Geophysics. 72, 152–168.

Maheswari, R.U., Boominathan, A. and Dodagoudar, G.R. 2010b. Use of Surface Waves in Statistical Correlations of Shear Wave Velocity and Penetration Resistance of Chennai soils. Geotechnical and Geology Engineering. 28, 119-137.

Marto, A., Soon, T. C., Kasim, F. and Suhatril, M. 2013. A Correlation of Shear Wave Velocity and Standard Penetration Resistance. Electronic Journal of Geotechnical Engineering. 18, 463-471.

Menke, W. 1984. Geophysical Data Analysis: Discrete Inverse Theory, revised ed. Academic Press Inc., New York, U.S.A. 289 pp.

Ohta, Y., Goto, N., Kagami, H. and Shiono, K. 1978. Shear wave velocity measurement during a standard penetration test. Earthquake Engineering and Structural Dynamics. 6, 43–50.

Palmer, D. 1980. The generalized reciprocal method of seismic refraction interpretation. Society of Exploration Geophysics, 104 pp.

Park, C.B., Miller, R.D. and Xia, J. 1999. Multichannel analysis of surface waves, Geophysics. 64, 800–808.

Richart, F.E., Hall, J.R. and Woods, R.D. 1970. Vibrations of Soils and Foundations. Prentice-Hall, Englewood Cliffs, New Jersey, U.S.A., 414 pp.

Saardsud, A. and Srisangjun, W. 2002. Geology of Hat Yai plane (5023 II), Department of Mineral Resources, DMR (in Thai).

Sawata, H., Wongsomsak, S., Tanchotikul, A., Dansawasdi, R., Maneeprapun, K. and Muenlek, S. 1983. A hypothetical idea on the formation of HatYai basin and the Songkhla lagoon. Proceedings of the Annual Technical Meeting 1982, Department of Geological Sciences, Chiang Mai University, Chiang Mai, Thailand, 109-120.

Seed, H.B., Idriss, I.M. and Arango, I. 1983. Evaluation of liquefaction potential using field performance data. Journal of Geotechnical Engineering. 109, 458–482.

Schwenk, J.T., Miller, R.D., Ivanov, J., Sloan, S. and McKenna, J. 2012. Joint shear wave analysis using MASW and refraction traveltime tomography. Proceeding of 25th Symposium on the Application of Geophysics to Engineering and Environmental Problems 2012 (SAGEEP 2012), Tucson, Arizona, U.S.A., March 25-29, 2012.

Sheriff, R.E. and Geldart, L.P. 1995. Exploration Seismology, Second Edition, Cambridge University Press, Cambridge, U.K., 592 p.

Signanini, P. and Torrese, P. 2004. Application of high resolution shear-wave seismic methods to a geotechnical problem, Bulletin of Engineering Geology and the Environment. 63, 329–336.

Sloan, S.D. Miller, R.D., McKenna, M.H. and McKenna, J.R. 2009. Using Shear-wave Velocity to Detect Void induced Changes in Stress, Proceeding of 15th European Meeting of Environmental and Engineering Geophysics, Dublin, Ireland, September 7-9, 2009.

Suto, K. 2011. Pseudo-N-value from the S-wave velocity- A proposal for communicating with the civil engineers. Proceeding of 73rd EAGE Conference and Exhibition, Vienna, Austria, May 23-26, 2011.

Sutiwanich, C., Hanpattanapanich, T., Pailoplee, S. and Charusiri, P. 2012. Probability seismic hazard maps of Southern Thailand. Songklanakarin Journal of Science and Technology. 34(4), 453-466.

Thitimakorn, T. and Channoo, S. 2012. Shear Wave Velocity of Soils and NEHRP Site Classification Map of Chiang Rai City, Northern Thailand. Electronic Journal of Geotechnical Engineering. 17, 2891-2904.

Tsiambaos, G. and Sabatakakis, N. 2011. Empirical Estimation of Shear Wave Velocity from In Situ Tests on Soil Formations in Greece. Bulletin of Engineering Geology and the Environment. 70, 291–297.

Turesson, A. 2007. A comparison of methods for the analysis of compressional, shear, and surface wave seismic data, and determination of the shear modulus. Journal of Applied Geophysics. 61, 83-91.

USGS 2013. United States Geological Survey. Available from: http://earthquake.usgs.gov/hazards/apps/vs30/custom.php. [September 19, 2013].

Uyanik, O., Ekinci, B. and Uyanik, N.A. 2013. Liquefaction analysis from seismic velocities and determination of lagoon limits Kumluca/Antalya example. Journal of Applied Geophysics. 95, 90-103.

Xia, J., Miller, R.D. and Park, C.B. 1999. Estimation of near-surface shear-wave velocity by inversion of Rayleigh waves. Geophysics. 64, 691–700.

Xia, J., Miller, R.D., Park, C.B., Wightman, E. and Nigbor, R. 2002. A pitfall in shallow shear-wave refraction surveying, Journal of Applied Geophysics. 51, 1–9.

Yordkayhun, S. 2011. Detecting near surface objects using seismic traveltime tomography: Experimentation at a test site. Songklanakarin Journal of Science and Technology. 33, 477–485.

Yordkayhun, S. Tryggvason, A. Norden, B., Juhlin, C. and Bergman, B. 2009. 3D seismic traveltime tomography imaging of the shallow subsurface at the CO2SINK project site, Ketzin, Germany. Geophysics. 74, G1–G15.

Youd, T.L. and Idriss, I.M. 2001. Liquefaction resistance of soils: summary report from the 1996 NCEER and 1998 NCEER/NSF workshops on evaluation of liquefaction of soils. Journal of Geotechnical and Geoenvironmental Engineering, 297-313.

Zhang, J. and Toksöz, M.N. 1998. Nonlinear refraction traveltime tomography. Geophysics. 63, 1726–1737.